

Hydrothermal system mapped by CSAMT on Karthala volcano, Grande Comore Island, Indian Ocean

Cécile Savin^{a,*}, Michel Ritz^b, Jean-Lambert Join^a, Patrick Bachelery^a

^a *Laboratoire des Sciences de la Terre, Université de la Réunion, BP 7151, 97715 Saint-Denis Messag. Cedex 9, France*

^b *IRD-UR Géophysique, BP 1386, Dakar, Senegal*

Received 27 June 2000; accepted 18 June 2001

Abstract

Controlled source audio-magnetotelluric (CSAMT) has been used to investigate the resistivity structure of the summit region of Karthala volcano. The major purpose of this CSAMT survey is to locate the active hydrothermal system. The presence of the hydrothermal system had already been inferred from surface evidence of hydrothermal activity and from self-potential (SP) mapping of the Karthala summit zone. The results of the 1D CSAMT inversion indicate the following: (1) a highly resistive (500–5000 Ω m) 200- to 400-m thick surface layer, that is characteristic of dry basaltic rocks, and made up of lava flows and/or tuff breccias; (2) a 300- to 1200-m thick layer of intermediate resistivity (20–400 Ω m), thought to be representative of the groundwater body; and (3) a deep conductor with a resistivity of less than 2 Ω m, which might be related to the active hydrothermal system.

This hydrothermal system appears to be bounded by caldera edges and shows the same north–south trend. Its depth ranges from more than 1 km to less than 0.7 km in the northern part of the caldera and its resistivity ranges from 2 to 0.5 Ω m in the northern part of the caldera. Less resistive zones and the shallowest depths of this conductive layer are well correlated with the largest SP positive anomalies and are assumed to be generated by hot fluid circulation. The most active hydrothermal zone is situated in the northern part of the caldera. © 2001 Elsevier Science B.V. All rights reserved.

Keywords: Karthala volcano; CSAMT method; Resistivity structure; Hydrothermal system

1. Introduction

In recent years, electromagnetic (EM) methods have become prominent tools for detailed structural resistivity studies, especially in volcanic regions where surface resistivity is high. The controlled source audio-magnetotelluric (CSAMT) method has

been successfully used for geothermal exploration (Bromley, 1993; Wannamaker, 1997) to overcome a lack of telluric signal strength in the audio-frequency portion of the natural spectrum.

We applied the CSAMT method to the Karthala volcano, which forms the southern two-thirds of the Grande Comore Island in the Indian Ocean between latitude 11–13°S and longitude 43–46°E (Fig. 1). This active basaltic shield volcano (2361 m a.s.l.) displays a typical Hawaiian structure, with two opposing rift zones diverging from a summit caldera,

* Corresponding author. Fax: +33-2-62-93-82-66.
E-mail address: savin@univ-reunion.fr (C. Savin).

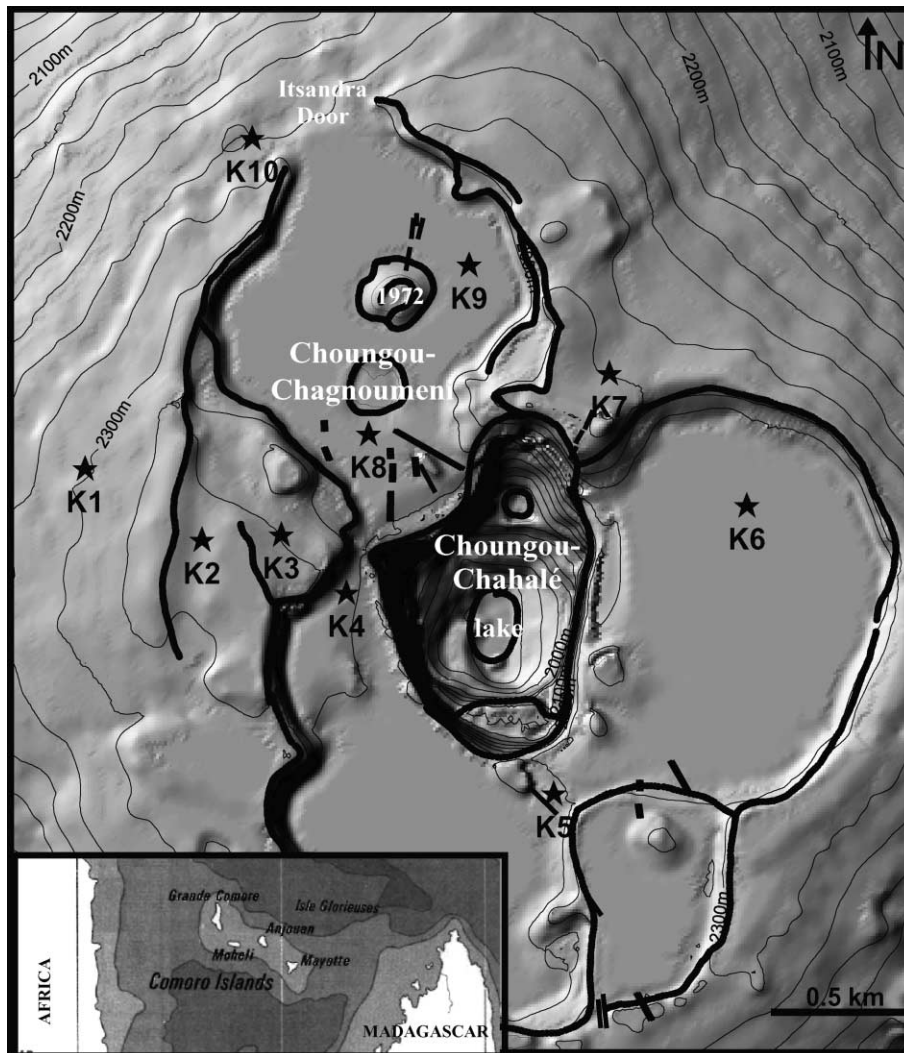


Fig. 1. Topography (reinforced by a shaded relief) and structural features (black lines) of the Karthala summit area (contour spacing: 25 m) showing the locations of the CSAMT sites (black stars). The lower box shows the location of the Grande Comore Island.

and a 290-m deep pit crater named “Choungou–Chahalé” lying in the center of the caldera (Fig. 1). At least eight eruptions have occurred during the 20th century. The Karthala eruptive style is mostly effusive, however phreatic and phreato-magmatic explosions have occurred in 1918, 1948, 1952 and 1991. The last one, which took place on the July 11, 1991, was purely phreatic, and formed a new crater (280 m in diameter, 43 m deep) in the bottom of the “Choungou–Chahalé”, which was partly filled by a lake that still exists today (Bachèlery et al., 1995).

The summit of Karthala volcano presents some surface evidence of hydrothermal activity: hydrothermal alteration affecting some sites located on caldera faults, active fumaroles in the “Choungou–Chagnoumen” (Fig. 1), an active solfatara (96 °C) called “soufrière” and located 2 km north of the caldera. Changes of the summit lake water level (metric order), not correlated with precipitation and involving a rise of the water table in a geothermal system, have also been observed between 1991 and 1997.

The geophysical investigations of the Karthala volcano have been very limited. Only a seismicity study (Savin, 1995) and self-potential (SP) measurements (Lénat et al., 1998) have been performed on the summit area. In addition, a few structural aspects have been inferred from the Karthala volcanic processes and from geological studies (Bachèlery and Coudray, 1990; 1993). These studies point to the presence of a very active hydrothermal system underneath the summit caldera. Consequently, a CSAMT survey was considered suitable for providing information about the electrical structure beneath the Karthala summit region, especially in regard to the location of the hydrothermal system.

2. CSAMT method

Controlled source audio-magnetotelluric method is a frequency-domain sounding technique that utilizes artificial and natural EM fields to measure resistivity variations in the ground. Goldstein and Strangway (1975) introduced the use of a controlled source to overcome the weak signals associated with the conventional audio-magnetotelluric (AMT) method. Typical CSAMT equipment consists of a transmitting station, the source of which is a dual horizontal electrical dipole, and a receiving station that measures the orthogonal horizontal components of the electric (E) and magnetic (H) fields. The relative phase shift between E and H yields the phase of the CSAMT impedance tensor. The ratio of E and H yields the apparent resistivity.

The interpretation of CSAMT data is more complicated than that of the AMT. This is due to the measurements of the EM fields which often have to be carried out in the near-field zone of the transmitter where the homogeneity of the EM fields is disturbed. CSAMT allows plane wave interpretation if the transmitter–receiver distance is greater than 3.5 skin depths. This allows the application of MT equations derived for a plane wave source. In traditional CSAMT surveys, only the far-field data have been interpreted using MT methods. More recently, modeling advances enable us to include near-field data in the interpretation (Boerner et al., 1993; Lu et al., 1997).

CSAMT measurements were recorded using the Stratagem tensor system of Geometrics. The transmitter operates in the frequency range of 500 Hz–92 kHz. For the lower frequencies (10–1000 Hz), the system uses the natural-source EM fields, similar to the AMT method. At the receiving site, two components of the electric field are measured with perpendicular dipoles using steel electrodes, whereas two components of the magnetic field are recorded with sensor coils. This procedure results in a tensor estimate of the impedance.

3. CSAMT measurements

During April 1998, CSAMT was applied to the summit region of the Karthala volcano. The 10 measurement sites are shown in Fig. 1. For each site, the controlled source transmitter was placed between 300 and 500 m from the receiving site, depending on the skin depth (close enough to obtain signal and far enough to enable plane wave interpretation). Due to the relatively rough terrain, it was difficult to perform more CSAMT measurements, resulting to little data obtained from the southern part of Karthala. The data was processed and the impedance tensor (Vozoff, 1972) was rotated to azimuths according to the determination of the electrical strike directions at each frequency for each site. Strike and cross-strike apparent resistivity and phase curves have been calculated from the impedance tensor that was obtained. At all sites except one (site 7), we found that the apparent resistivities in both directions were relatively isotropic through the observed bandwidth. This implies that geological surface layers are homogeneous on a large scale. The data are insensitive to rotation angle. Adjacent sites show similarities, the main difference being the position of the maximum rate in apparent resistivity, which is characteristic of the depth of the high resistivity in dry basaltic rocks. This maximum is generally within the frequency range of 10^4 – 10^3 Hz. At all sites, the CSAMT estimates are characterized by a decrease in apparent resistivity with decreasing frequency at the end of the measurement range. This indicates the presence of a deeper conductive layer. Examples of CSAMT sounding curves are given in Fig. 2.

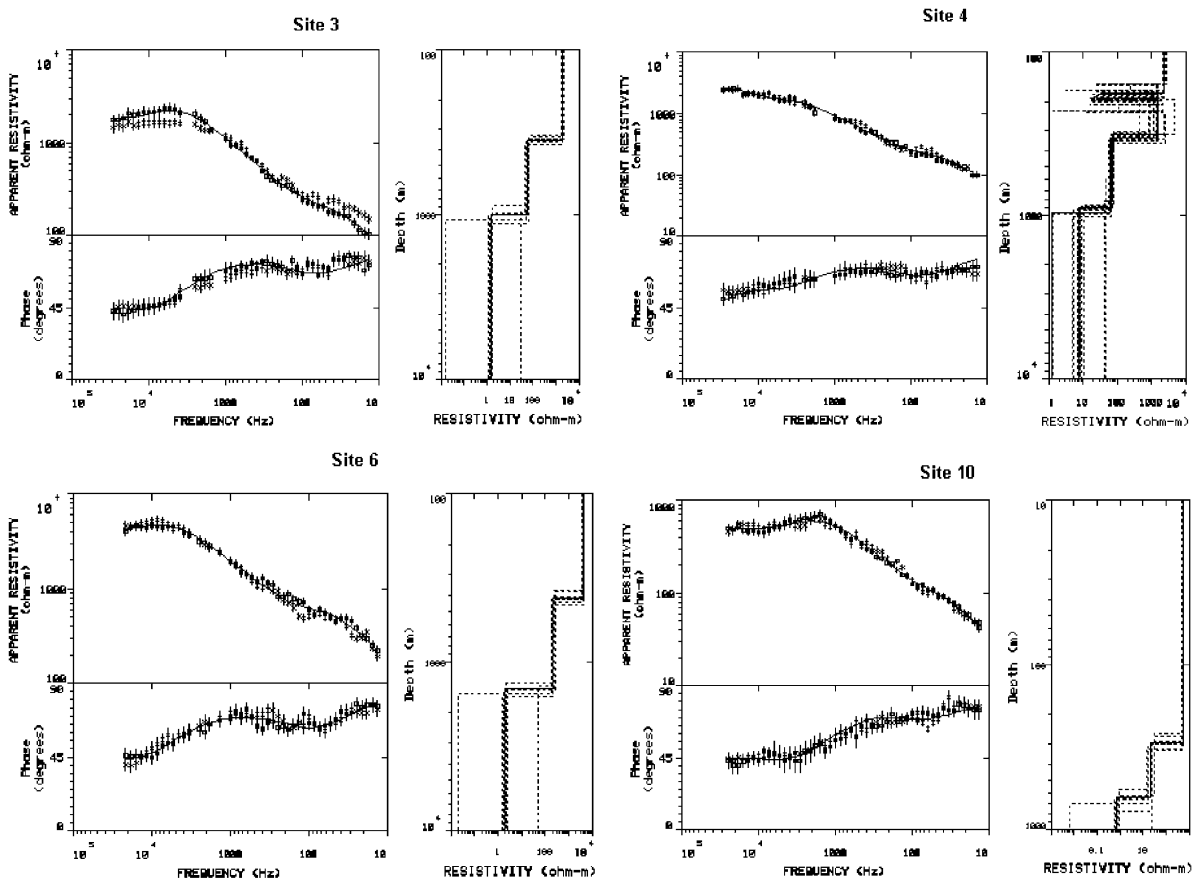


Fig. 2. Examples of CSAMT soundings for sites 3, 4, 6 and 10 (Fig. 1). Solid squares and cross with error bars denote the observed values for strike and cross-strike direction, respectively. Solid lines (in the left-hand graph) show the calculated responses for the best-fit models shown in the right-hand graph. Dashed lines are the equivalent models.

Generally, the sounding data are approximately 1D in nature, as shown in Fig. 2, except at site 7 where a static shift (Berdichevsky and Dimitriev, 1976) due to local, near-surface non-homogeneities has been observed (Fig. 3). The static-effect distortion consists of a parallel splitting of the two observed mode curves and may lead to false interpretation (Pellerin and Hohmann, 1990). A number of techniques has been proposed to attenuate this effect as, for instance, the use of near-surface resistivity data obtained with independent geophysical methods (Sternberg et al., 1988). Unfortunately, no other resistivity information was available on Karthala volcano. However, the existence of the crater complex “Choungou–Chahalé” (Fig. 1), close to the CSAMT

sites, can provide a frame for the choice of a mode at site 7 for the 1D interpretation. In fact, at the bottom of the central crater, formed during the phreatic eruption of 1991, the aquifer is present at an elevation of 1920 m. This is suggestive of a deep conductive medium underneath several volcanic flows.

4. Modeling

1D models (Interpex, 1993) have been adjusted to the apparent resistivity and phase curves at each site. The data were interpreted using the minimum number of concordant layers. This typically resulted in a

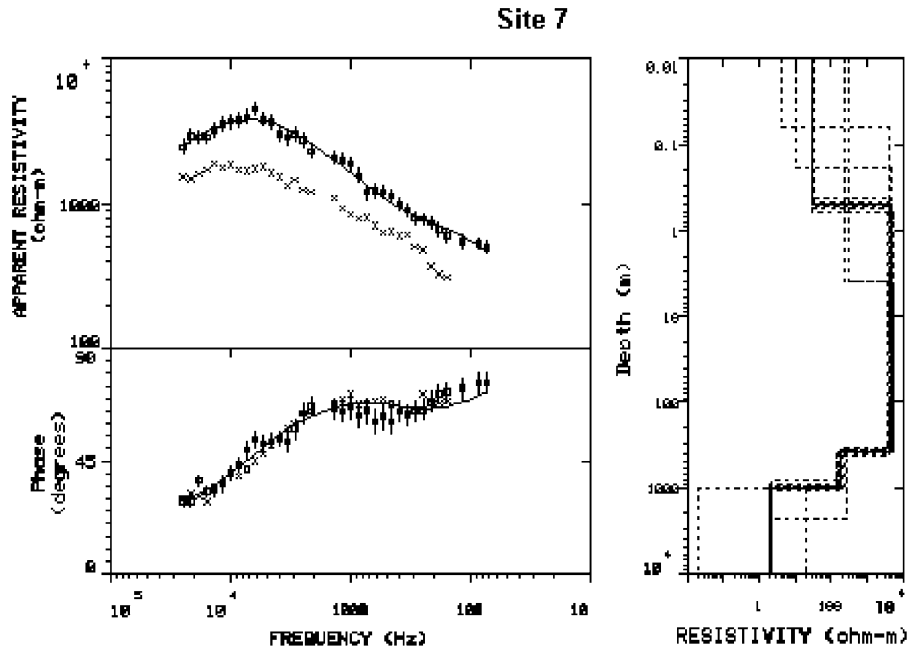


Fig. 3. Example of CSAMT soundings for site 7 showing static shift. Solid squares and cross with error bars denote the observed values for strike and cross-strike direction, respectively. Solid lines (in the left-hand graph) show the calculated responses for the best-fit models shown in the right-hand graph. Dashed lines are the equivalent models.

model with three major layers. Fig. 2 depicts four examples of 1D models to data matches, as well as the inferred electrical resistivity structure beneath each site.

Generally, the results of the layered inversion indicate the following resistivity properties of the summit region of the Karthala volcano.

(1) A highly resistive (500–5000 Ω m) 200- to 400-m thick surface layer that can be locally subdivided into two units at sites 4, 5 and 8 (see the example for site 4 in Fig. 2), where additional conductive layers of some tens of Ω m (2–4 m thick) appear due to the high resolution of CSAMT method, in the interior of this resistive layer at a depth of about 150 m.

(2) A second layer (300–1200 m thick) with intermediate resistivity values of about 20–400 Ω m. Resistivity rates lower than 40 Ω m are found beneath sites 5, 8, 9 (not shown) and 10 along an almost north–south central axis in the caldera and are confined within a thinner layer of 450 m or less,

except for site 5, in the southern part of Karthala, where thickness is greater than 700 m.

(3) A conductor with resistivity rates of less than 2 Ω m (except site 1 whose resistivity is 11 Ω m). In the northern part of the study area, resistivities of less than 0.8 Ω m have been found.

In order to better determine the geoelectric structure of the Karthala summit zone, a 2D elevation contour map of the uppermost of intermediate resistivity and the conductive layers was computed, based on the 1D models for each site, as shown in Fig. 4a and b, respectively. For the intermediate-resistivity layer (Fig. 4a), the top elevation is about 1950 ± 50 m for each site, except for site K6 (deeper) and sites K2 and K8 (shallower), involving a general deepening of this layer from the western to the eastern part of the caldera. Note that the 2D model limits the lake level to between 1920 and 1940 m in height, which describes precisely the reality. On the other hand, the deeper conductive layer (Fig. 4b) has a general north–south elongation with a deepening of each

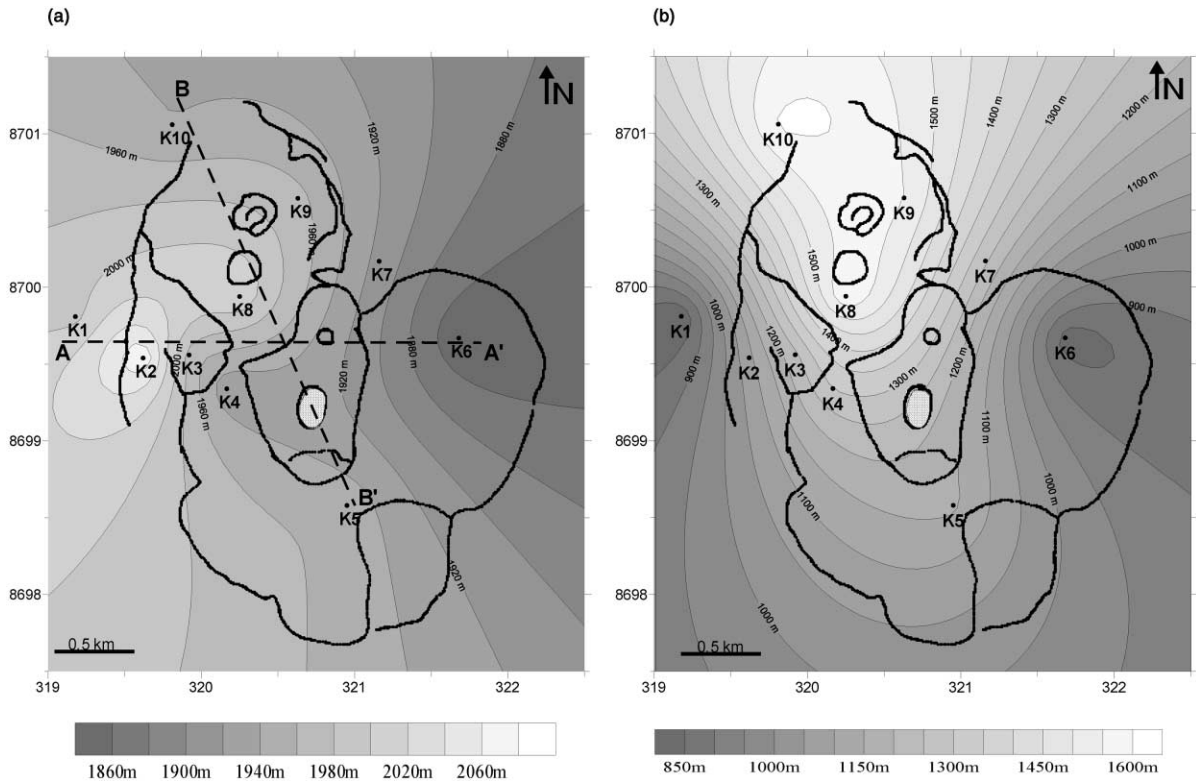


Fig. 4. Elevation contour map in meters (above sea level) of the intermediate resistivity (a—intervals = 20 m) and the conductive (b—intervals = 50 m) layers as determined from CSAMT data. Black lines show the main structural features. CSAMT site locations are indicated. X and Y represent the UTM coordinates (in km).

side along a W–E profile across the caldera and a relatively high elevation in the northern part of the caldera.

5. Discussion

The application of the CSAMT method at the Karthala volcano summit zone reveals three layers of different electrical resistivities: a resistive surface layer, an intermediate-resistivity layer and a conductor (Fig. 5).

The first resistive (500–5000 Ω m) layer obtained for all models is typical for dry basaltic rocks (Courteaud et al., 1997). For some sites (sites 4, 5 and 8), the models suggest additional thin (< 4 m) conductive layers of some tens of Ω m that can be interpreted as accumulation zones of pyroclastic ashes

i.e., as coming from the paroxysmal phreato-magmatic eruption of –4000 B.P. (Bachèlery and Coudray, 1993).

Moderate resistivities (20–400 Ω m) computed for all sites are too low to indicate dry basaltic rocks and can be interpreted in terms of water content in the second layer. This means that this layer represents the groundwater body developed in basaltic rocks (Descloitres et al., 1997). Resistivity variations within this layer may indicate variations in the relative contribution of clay interbeds in the section (Lienert, 1991). Drawing from the hydrological model of the Piton de la Fournaise volcano, Reunion Island (Folio et al., 2000), we assume that the top of the second layer is representative of the piezometric surface (Fig. 5). This hypothesis is consistent with the geophysical interface, close to the water level of the lake (see Fig. 5b). The piezometric slope is

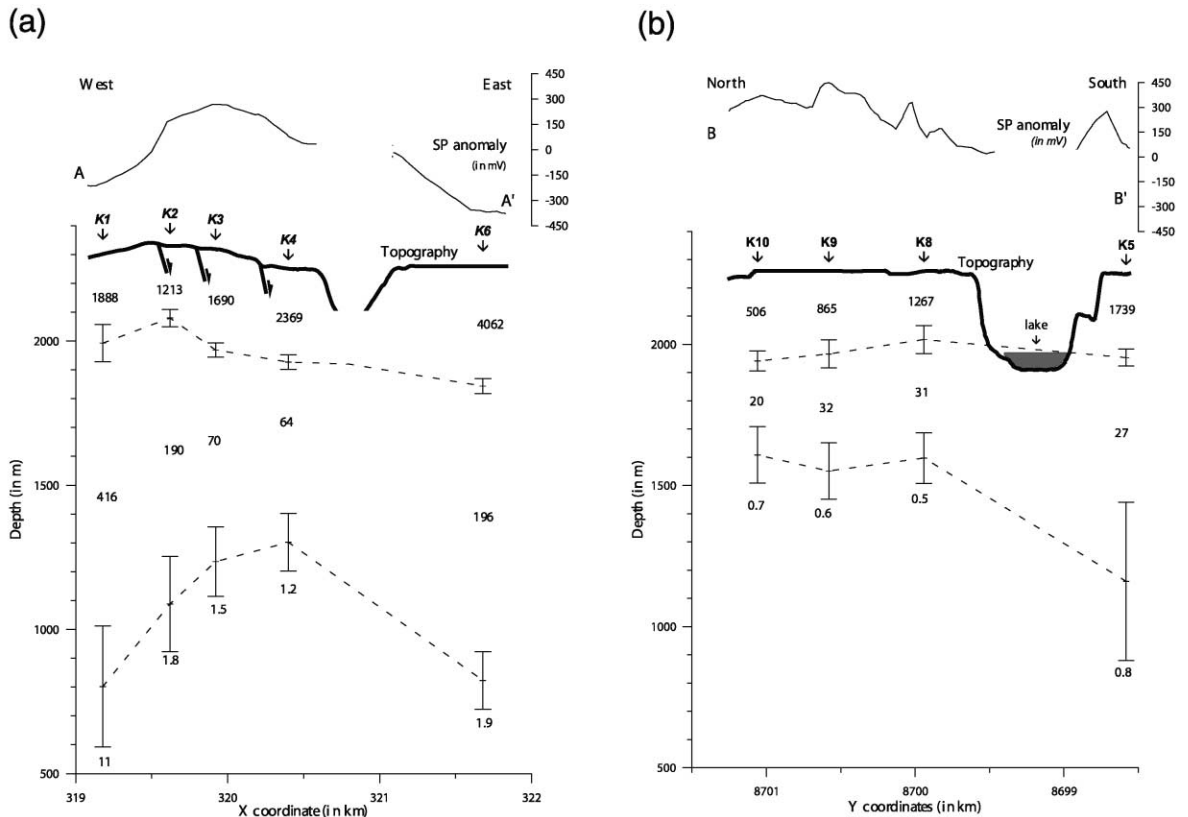


Fig. 5. Cross-sections showing resistivity models obtained with the 1-D inversion from CSAMT sites (resistivity is in Ω m). Error bars are estimated from equivalent models (see Fig. 2). Black lines indicate the topography along the profile. SP anomaly variations along the profile are also shown in the upper part of the graph. (a) Profile AA' (see Fig. 4a) crossing K1, K2, K3, K4 and K6 CSAMT sites; (b) profile BB' (see Fig. 4a) crossing K5, K8, K9 and K10 CSAMT sites.

traced by this geophysical interface (see Figs. 4a and 5a). This implies a groundwater recharge in the western part of the caldera as a result of a precipitation maximum in the western flank of the volcano (Battistini and Verin, 1984).

Considering the known presence of an active hydrothermal system at Karthala volcano and the typically very low resistivity values ($\ll 10 \Omega$ m) obtained for geothermal and hydrothermal systems (Haak et al., 1989; Sainato et al., 1993; Hoover et al., 1984), the boundary between the second layer and the deep conductor can be interpreted as a mark of the top of the active hydrothermal system. The CSAMT survey allows us to model its geometry (Figs. 4b and 5). In fact, the CSAMT model infers

an average depth of 1000 m for the top of the hydrothermal system, or, more precisely, a variation from about 1500-m depth beneath the east and west sides of the caldera (sites K1 and K6) to nearly 700 m beneath the north part of the caldera (sites K8, K9 and K10) (see Fig. 5).

Causes for conductive conditions include (i) high temperature, (ii) low-resistivity pore water, (iii) increasing porosity, (iv) conducting mineralization, and (v) hydrothermal alteration (Mogi and Nakama, 1993). In hydrothermal zones, conducting mineralization and hydrothermal alteration are intimately linked but the major influence on resistivity values seems to be temperature. On the other hand, the modeling procedure, which has been used for all

CSAMT sites, produces a structure composed of discrete layers, but it is likely that in reality, a gradual decrease in resistivity over some finite depth range can be found (Ingham, 1992). Thus, the apparently shallower depth of the deeper conductive material ($< 0.8 \Omega \text{ m}$) beneath sites 8, 9 and 10 in the northern part of the caldera (Fig. 5b) can be interpreted as being due to higher-than-normal temperatures for such depths, as well as to the more active upward fluid circulation related to fumarole activity around the Choungou–Chagnoumeni pit-crater. On the contrary, the greater depth of the conductive

layer at sites 1 and 6 (Fig. 5a) indicates the east–west boundaries of the hydrothermal system and a weaker temperature gradient. Likewise, spatial variations of the geothermal gradient can also explain the resistivity variations of the intermediate-resistivity layer.

The presence of this hydrothermal system has already been inferred from the surface evidence of hydrothermal activity, as described in the Introduction. Second, an SP map of the summit zone of the Karthala volcano (Fig. 6) was obtained from about 1300 measurements effectuated inside the caldera during December 1995 and October 1996 (Lénat et

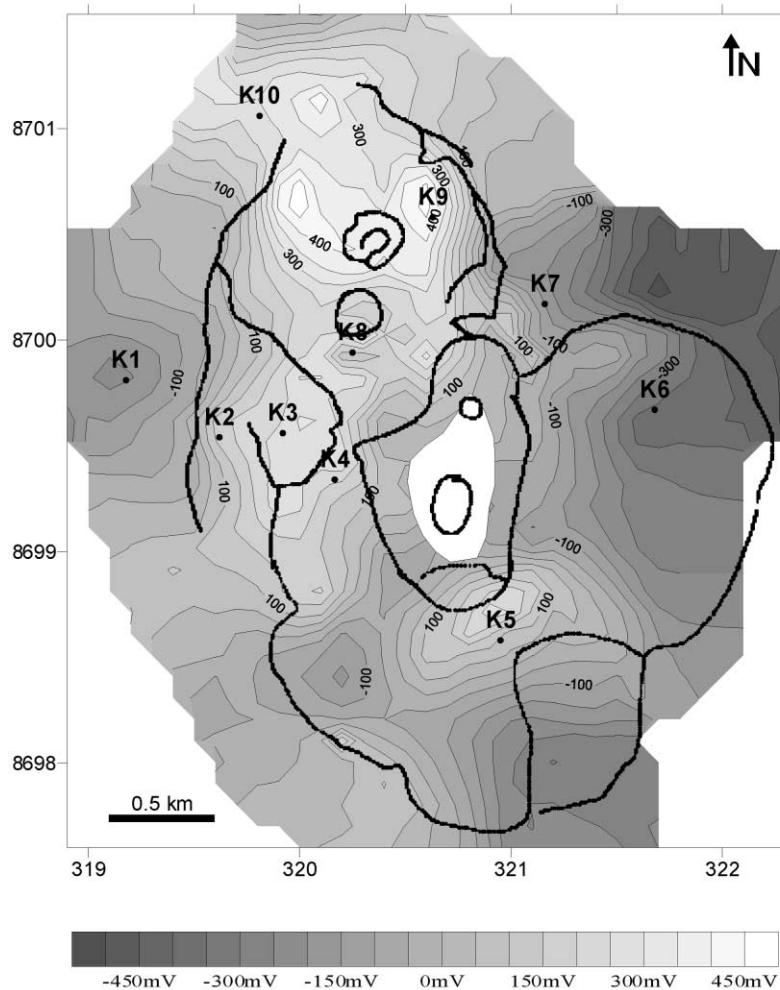


Fig. 6. SP map of the Karthala summit zone (adapted from Lénat et al., 1998). Contour spacing: 50 mV. Thick lines denote the main structural features. CSAMT site locations are indicated. X and Y represent the UTM coordinates (in km).

al., 1998). A significant large positive anomaly (up to 400 mV) was observed in the northern part of the caldera (Fig. 6) showing that the greatest hydrothermal activity was not centered on the main Choungou–Chahalé crater, as might have been expected. Note, SP anomalies are generated by fluid flow, heat and ions in the Earth's interior, and SP investigations have been used to locate and delineate sources associated with such flows in geothermal areas (Corwin and Hoover, 1979).

In comparing CSAMT and SP results (Figs. 4 and 6), a good correlation exists between SP positive anomalies and low-resistivity zones ($< 0.8 \Omega \text{ m}$). Lénat et al. (1998) interpreted the three main SP positive anomalies observed in the northern, eastern and southern parts of the caldera (Fig. 6) as indicative of the presence of heat sources and the occurrence of hydrothermal processes. The application of the CSAMT method provides information about the depth location of this hydrothermal system and enables us to differentiate the origin of the different SP anomalies. We can observe that the SP positive anomaly in the northern part of the caldera is clearly well correlated with the most active hydrothermal zone inferred from CSAMT models. This, however, is not so evident for the two other positive anomalies. The eastern SP positive anomaly seems to indicate the shallowest depth of the water table better, whereas the southern anomaly, interpreted as a secondary hydrothermal active zone (Lénat et al., 1998), seems to be influenced both by the hydrothermal active system and also by the water-saturated medium and the high level of the water table.

In addition to the influence of hydrothermal circulation, the SP measurements seem to be influenced by groundwater circulation from west to east, calibrated by the piezometric gradient of the top of the intermediate-resistivity layer (Fig. 5a), which is known to be representative of the piezometric surface.

6. Conclusion

The CSAMT method, applied to the Karthala volcano, enabled us to determine the structure of the first kilometers of the summit area, which in electri-

cal terms can be divided into three ranges of resistivity values: (1) a highly resistive (500–5000 $\Omega \text{ m}$), 200- to 400-m thick surface layer, which is characteristic of dry basaltic rocks and mainly constituted by lava flows and/or tuff breccias; (2) an intermediate-resistivity (20–400 $\Omega \text{ m}$), 300- to 1200-m thick layer, interpreted to be representative of the groundwater body; and (3) a deep conductor with a resistivity of less than 2 $\Omega \text{ m}$, which might be related to the active hydrothermal system.

The two geophysical interfaces highlighted by the CSAMT method do not have the same origin. The first one is assumed to represent a hydrogeological interface controlled by the volcano's topography, precipitation rate and spatial distribution. The second interface may mark the top of the hydrothermal system and is probably better imagined as a continuous decrease of resistivity related to increasing heat, conducting mineralization and hydrothermal alteration with depth.

The major purpose of this CSAMT survey is to define the location of the active hydrothermal system of the Karthala volcano: it appears to be bounded within the caldera and possesses the same north–south elongation; its depth ranges from more than 1 km to less than 0.7 km in the northern part of the caldera; its resistivity values range from 2 to 0.5 $\Omega \text{ m}$ in the northern part of the caldera. Less resistive zones and the shallowest depths of this conductive layer are well correlated with the largest SP positive anomalies and can be assumed to be generated by the same source, i.e. hot fluid circulation.

Acknowledgements

Thanks to T. Mogi, an anonymous reviewer, Bernard Robineau, Sirit Coeppicus and Phil Sills for constructive criticism and help in improving the manuscript. Without Ali Youssef and the many other Comoran carriers, this CSAMT survey would not have been successful. This study was financed by the Laboratoire des Sciences de la Terre de l'Université de la Réunion, and Mission Française de Coopération on Comore Island and the CNDRS (Grande Comore Island). C. Savin is financed by a Reunion Island Regional Grant.

References

- Bachèlery, P., Coudray, J., 1990. La grande Comore et son volcan actif: le Karthala. Aspects géologiques, caractéristiques et évolution de l'activité volcanique. *J. Nat.* 2 (1), 32–48.
- Bachèlery, P., Coudray, J., 1993. Carte volcano-tectonique de la Grande Comore (Ngazidja) au 1/50000 avec notice explicative. Ed. Mission Française de coopération aux Comores.
- Bachèlery, P., Ben Ali, D., Desgrolard, F., Toutin, J.P., Coudray, J., Cheminée, J.L., Delmond, J.C., Klein, J.L., 1995. L'éruption phréatique du Karthala (Grande Comore) en Juillet 191. *C. R. Acad. Sci. Paris, Ser. Ila* 320, 691–698.
- Battistini, R., Verin, P., 1984. Géographie des Comores. Ed. Nathan, France, 142 pp.
- Berdichevsky, M.N., Dimitriev, V.I., 1976. Basic principles of interpretation of magnetotelluric sounding curves. In: Adam, A. (Ed.), *Geoelectric and Geothermal Studies*. Akademiai Kiado, Budapest, pp. 165–221.
- Boerner, D.E., Wright, J.A., Thirlow, J.G., Reed, L.E., 1993. Tensor CSAMT studies at the Buchans Line in central Newfoundland. *Geophysics* 58, 12–19.
- Bromley, C., 1993. Tensor CSAMT study of the fault zone between Waikite and Te Kopia geothermal fields. *J. Geomagn. Geoelectr.* 45, 887–896.
- Corwin, R.F., Hoover, D.B., 1979. The self-potential method in geothermal exploration. *Geophysics* 44 (2), 226–245.
- Courteaud, M., Ritz, M., Robineau, B., Join, J.L., Coudray, J., 1997. New geological and hydrogeological implications of the resistivity distribution inferred from audiomagnetotellurics over La Fournaise young shield volcano (Reunion Island). *J. Hydrol.* 203, 93–100.
- Folio, J.L., Join, J.L., Robineau, B., Coudray, J., Ritz, M., 2000. Complementarity of electromagnetic prospecting and groundwater modelling to study shield volcano hydrogeology: Piton de la Fournaise volcano case study, Reunion Island. In: Siliilo, O., et al. (Eds.), *Groundwater: Past Achievements and Future Challenges*. Balkema, Rotterdam, pp. 385–388, ISBN 90 5809 159 7.
- Goldstein, M.A., Strangway, W.D. et al., 1975. Audio-frequency magnetotellurics with a grounded dipole source. *Geophysics* 40, 669–683.
- Haak, V., Ritter, O., Ritter, P., 1989. Mapping the geothermal anomaly on the island of Milos by magnetotellurics. *Geothermics* 18 (4), 533–546.
- Hoover, D., Rodrigues da Silva, A., Pierce, H., Amaral, R., 1984. The application of audio-magnetotelluric surveys on São Miguel island, Azores, Portugal. *Geotherm. Resour. Counc.*
- Ingham, M., 1992. Audiomagnetotelluric soundings on White Island volcano. *J. Volcanol. Geotherm. Res.* 50, 301–306.
- Interpex 1993. EMIX MT User's Manual: Magnetotelluric Data Interpretation Software.
- Lénat, J.F., Robineau, B., Durand, S., Bachèlery, P., 1998. Etude de la zone sommitale du volcan Karthala (Grande Comore) par polarisation spontanée. *C. R. Acad. Sci. Paris* 327, 781–788.
- Lienert, B.R., 1991. An electromagnetic study of Maui' last active volcano. *Geophysics* 56, 972–982.
- Lu, X., Unsworth, M.J., Booker, J.R., 1997. Two dimensional inversion of tensor CSAMT data. *Proc. 67th Ann. Internat. Mtg., Soc. Expl. Geophys.*
- Mogi, T., Nakama, S., 1993. Magnetotelluric interpretation of the geothermal system of the Kuju volcano, southwest Japan. *J. Volcanol. Geotherm. Res.* 56, 297–308.
- Pellerin, L., Hohmann, G.W., 1990. Transient electromagnetic inversion: a remedy for magnetotelluric static shifts. *Geophysics* 55, 1242–1250.
- Sainato, C.M., Febrer, J.M., Pomposiello, M.C., Mamani, M., Maidana, A., 1993. Magnetotelluric study of the Tuzgle volcano zone, Jujuy province, Argentina. *J. Geomagn. Geoelectr.* 45, 787–803.
- Savin, C., 1995. Comportement sismique et activité phréatique d'un volcan: le Karthala (île de la Grande Comore). Mémoire de DEA de l'Université J. Fourier, Grenoble, France.
- Sternberg, B.K., Washburne, J.C., Pellerin, L., 1988. Correction for the static shift in magnetotellurics using transient electromagnetic soundings. *Geophysics* 53, 1359–1468.
- Vozoff, K., 1972. The magnetotelluric method in the exploration of sedimentary basins. *Geophysics* 37, 98–141.
- Wannamaker, P.E., 1997. Tensor CSAMT survey over the Sulphur Springs thermal area, Valles Caldera, New Mexico, USA: Part I. Implications for structure of the western caldera. *Geophysics* 62, 451–465.